SUPPLEMENTAL MATERIAL

STATIONARITY

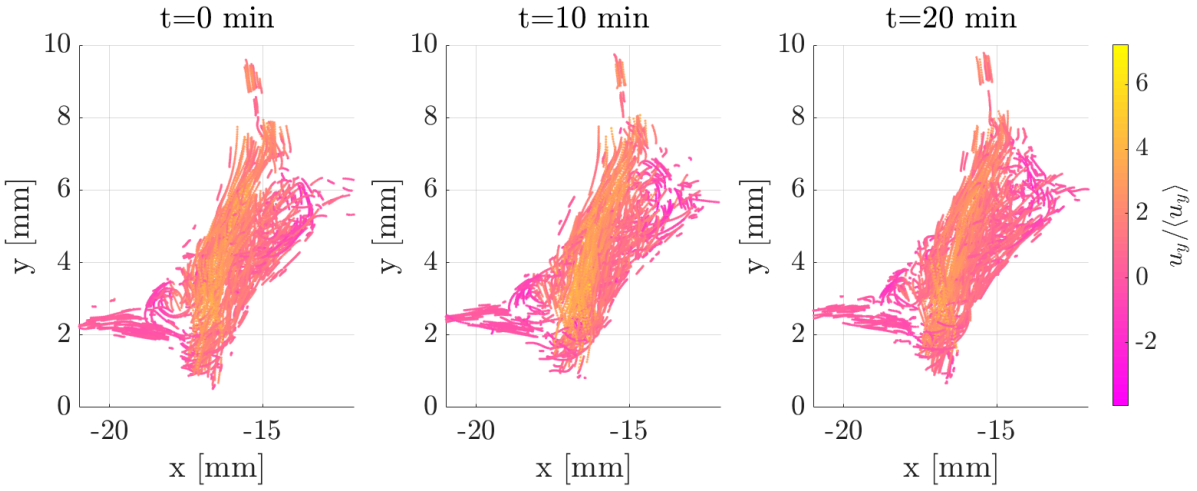

FIG. 1. 2-second timelapse of the Lagrangian velocity field inside a generic pore ($Re = 216$). The measurements were started 10 minutes apart, and the velocity field does not significantly change in time. Figures show the streamwise velocity u_y field normalized by the mean velocity (the average done over all the trajectories) $\langle u_y \rangle$

In order to study stationarity, we start by showing in figure 1, for the case Re=216, the superposition of all trajectories passing through the same bed, at the same generic pore, for three 2 seconds time-lapsed individual acquisitions. The measurements were started ten minutes apart from each other ($t = [0, 10, 20]$ min). The limited white sections correspond to four different surrounding beads. It can be qualitatively seen that the paths of the trajectories and the overall global structure of the flow is very robust and do not significantly vary, neither at the scale of the individual 2 seconds measurements, nor over much longer timescales (of the order of 20 minutes) when comparing the three cases.

For comparison, the characteristic time of the integral length T_L defined in terms of σ_u and L, is $T_L = L/\sigma_u = 0.2$s for the Re=216 case shown in figure 1.

In order to address more quantitatively the variability of the flow and better account for the possibly short time variations of the velocity, for each of the three measurements at [0, 10 and 20] min we have considered the binning of the measurement volume in 150x150x25 voxels. We then compute for all components of velocity the standard deviation of the temporal fluctuations of the velocity in each individual voxel $\sigma^t_{u_i}(x, y, z)$ over the 2 seconds (which roughly corresponds to 10 integral timescales) of duration of each measurement. We then define the rate of temporal variability, τ_{var}, as the ratio of the spatial average of this field of temporal fluctuations and the global standard deviation of the velocity σ_{u_i} (taken as the standard deviation of the velocity considering the ensemble of all velocities at every time for all the trajectories of each measurement) : $\tau_{var} = \langle \sigma^t_{u_i}(x, y, z) \rangle_{x,y,z} / \sigma_{u_i}$. We have also estimated the same variability parameter when all 3 measurements (spanning 6 seconds of measurements spread over 20 minutes of experiment) are merged together. We find that for the individual 2-second measurements $\tau_{var} \sim 13\%$, and $\tau_{var} \sim 15\%$ when all three measurements are merged. Note that this is an upper bound of the actual temporal fluctuation level, as some spatial variability due to the finite extent of the voxels (required to have sufficient trajectories per voxel and statistical convergence tends to increase the estimate of $\sigma^t_{u_i}(x, y, z)$.

This confirms the visual impression that the temporal variability of the trajectories is small and that most (more than 85%) of the variability of the reported velocity fluctuations arise from the spatial structure of the flow. This is drastically different from classical fluid turbulence, which is intrinsically driven by spatio-temporal fluctuations of equivalent magnitude. We call this situation quasi-frozen turbulence.

CORRELATION FUNCTIONS

In order to compute the correlation lengths, the correlation functions $\mathcal{R}$ are needed. They are defined as

$$\mathcal{R}_{ij} = \langle u_i'(\mathbf{x}+\mathbf{r}) u_j'(\mathbf{x}) \rangle.$$

They tend to one when $r = 0$ and two elements of fluid are no longer correlated at distances r when $\mathcal{R}_{ij} = 0$, which is the correlation length L. The computed correlation functions are shown in figure 2, and a dashed black line is shown at $\mathcal{R}_{ij} = 0$ for visualization purposed. Both $\mathcal{R}_{xx}$ and $\mathcal{R}_{yy}$ tend to one at $r = 0$ and become zero at different correlation lengths that depend on the Reynolds number and the component of the velocity that is being taken into account (see figure 4 in the Letter). Once they cross zero a slight oscillating pattern is observed, which is due to the presence of the beads. This shows that there is still a slight correlation present that oscillates spatially.

The crossed correlation function (fig. 2*c)*) shows that u_x and u_y are slightly correlated at $r = 0$ ($\mathcal{R}_{xy}(r = 0) \approx 0.25$) and the correlation remains low for all separation distances.

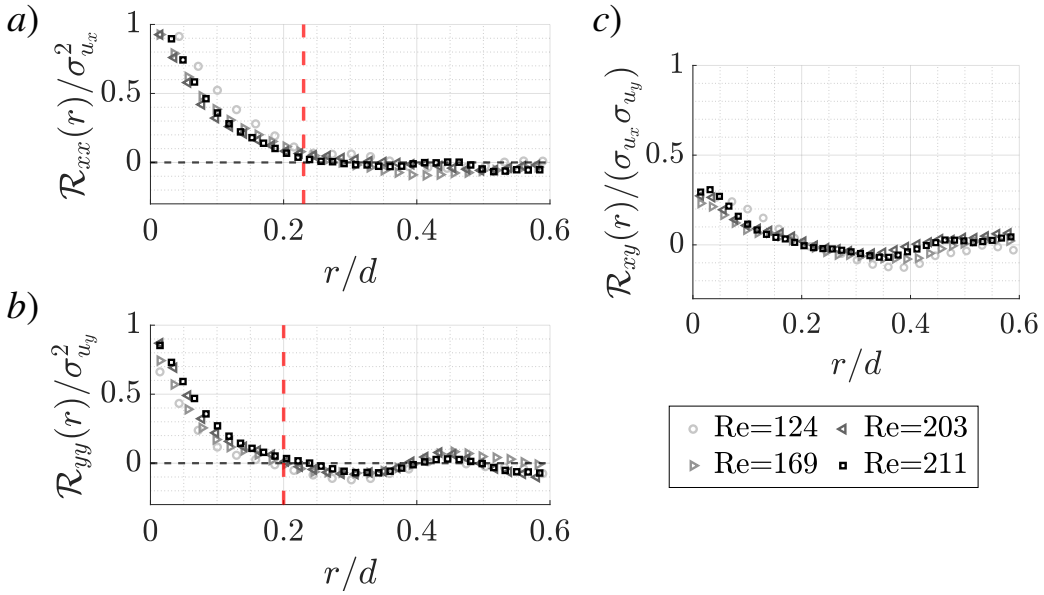

FIG. 2. Transversal and longitudinal structure functions (a) and b) respectively), normalized by their respective standard deviations. For reference, a horizontal line at zero is marked with a black dashed line and the vertical red dashed line shows the approximate point where $\mathcal{R}$ crosses zero. Subfigure c) shows the crossed correlation function.

TYPICAL PORE LENGTH

Here we provide a rough estimate of the typical pore length, by considering simple geometrical arguments. Let us have three spheres of radius $d/2$ closely packed together, as shown in figure 3. The three centers are joined by a triangle, and the typical pore length is shown in the plot as L_{pore}. The other relevant lengths are also shown as d (the sphere diameter) and $R = d/2$ the sphere radius. By making use of Pythagoras's theorem we have $L_{pore} = d/\sqrt{2} - d/2$, and the size of a typical pore is $L_{pore} \approx 0.2d$, which is of the order of magnitude of the computed correlation lengths. It is also consistent with figures 2*a* and *b*, at the point where the correlation becomes zero.

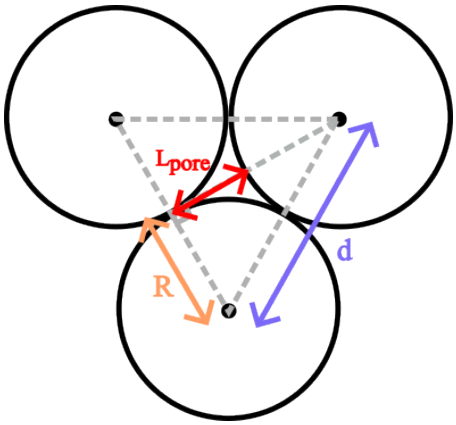

FIG. 3. Geometrical estimate of the typical pore length. d is the sphere diameter, R its radius and L_{pore} the typical pore scale. L_{pore} can be calculated using Pythagoras's theorem.

KOLMOGOROV'S CONSTANT

The Kolmogorov constant C_2 can be estimated by fitting the power law scaling for S_2 at inertial scales. To do so, we follow here the classical method used in turbulence, which consists in plotting the compensated structure function $S_2(r)/(\epsilon r)^{2/3}$. This requires to know *a priori* the value of the energy dissipation rate, which has been obtained here from the inertial range value of the crossed velocity-acceleration structure function S_{au}. Figure 4(Left) shows the compensated structure function for the different experiments (at different superficial velocities) explored here. The inertial range scaling appears as a plateau giving the value of C_2. Note that we consider here the total structure function $S_2 = (2S_{2x} + S_{2y})/3$. Figure 4(Right) shows the value of C_2, estimated as the average of the plateau over the range of scales $r/d < 0.1$; the errorbars correspond to the standard deviation of the plateau over the same range.

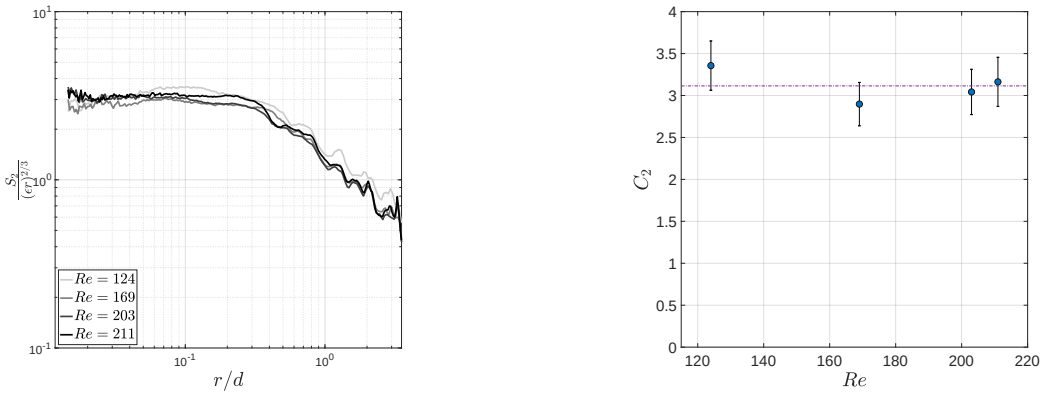

FIG. 4. (Left) Compensated total second structure function $S_2(r)/(\epsilon r)^{2/3}$. (Right) Estimated value of the Kolmogorov constant C_2 (the dashed represents the mean of all four values of C_2).